The origin of radiation tolerance in amorphous $Ge_2Sb_2Te_5$ phase-change random-access memory material

Konstantinos Konstantinou[a,1], Tae Hoon Lee[a], Felix C. Mocanu[a], and Stephen R. Elliott[a]

[a] Department of Chemistry, University of Cambridge, Lensfield Road, Cambridge CB2 1EW, UK.

[1] To whom correspondence may be addressed. E-mail: kk614@cam.ac.uk

Supporting Information

Modelling of a radiation-damage cascade corresponds to an example of simulation in which it is desirable to study an approach of an initially non-equilibrium system to equilibrium. As shown in Ref. (1), this type of problem can be investigated by using stochastic boundary conditions derived from the generalized Langevin equation by Kantorovich and Rompotis (2). In this approach, the system of interest is divided into two regions: (a) the internal atoms move according to Newtonian dynamics; and (b) a buffer region of atoms which are governed by Langevin equations of motion. In Langevin dynamics (3), the temperature is maintained through the following equations of motion:

$$\dot{r_i} = p_i/m_i \qquad \dot{p_i} = F_i - \gamma_i\, p_i + f_i,$$

where F_i is the force acting on atom *i* due to the interaction potential, γ_i is the friction coefficient and f_i is the random force with dispersion σ_i related to the friction coefficient via:

$$\sigma_i^2 = 2\, m_i\, \gamma_i\, k_B\, T/\Delta t$$

with Δt being the time-step used in the MD to integrate the equations of motion. It can be noted that Langevin dynamics are identical to a classical Hamiltonian in the limit of vanishing γ_i (3). The role of the atoms in the temperature-scaled Langevin region around the outer perimeter of the periodic-boundary-conditions is to dissipate heat without the need to actively scale the velocities of any atoms directly involved with the cascade interactions (4). Thus, the Newtonian region should include all atoms relevant to the process under study. In ion-irradiation simulations, the NVE thermodynamic ensemble is the correct approach to deal with the collisional phase in the Newtonian region.

Since the stochastic boundary-condition model follows directly from the generalized Langevin equation description and can perform as a correct NVT thermostat, this approach is a method of choice if one wants to do non-equilibrium molecular-dynamics simulations correctly. Performing molecular-dynamics with such a set-up guarantees that the system, which is out of equilibrium initially, is able to arrive at the appropriate canonical distribution.

To summarize, **Fig. S1** describes the simulation set-up used in our study to model ion irradiation based on the stochastic boundary-condition approach and performing mixed NVE Born-Oppenheimer and NVT Langevin *ab initio* molecular-dynamics. It is noted that the friction coefficient for the Langevin dynamics equations of motion was set equal to 10^{-2} fs^{-1}, which is a value typically used in MD simulations of amorphous materials, compensating between accuracy and performance.

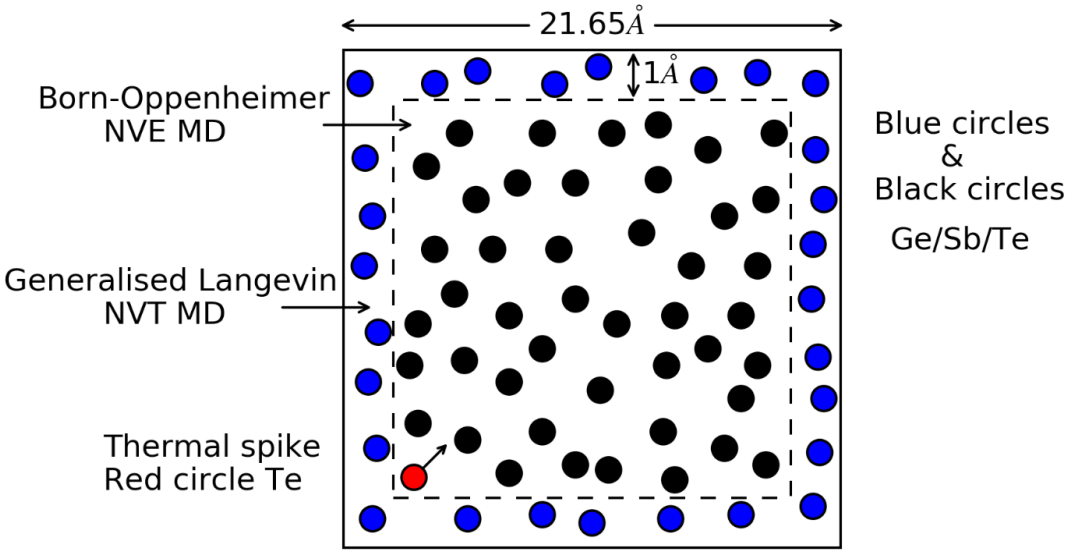

Fig. S1. Schematic overview of the simulation set-up used for the modelling of ion irradiation in amorphous $Ge_2Sb_2Te_5$. The simulation box was divided into two thermal regions. The atoms inside the 1 Å layer at the edges of the periodic-boundary-condition supercell undergo Langevin dynamics (NVT), whereas those outside it undergo Born-Oppenheimer molecular-dynamics (NVE). The outer layer corresponds to the heat-dissipation region, which drives the system to equilibration during the radiation-damage cascade, and acts as a heat-sink, preventing the kinetic disturbances from re-entering the simulation box. The primary knock-on atom (Te), highlighted as a red circle, was fired along the body diagonal of the simulation cell.

The CP2K code was used for the first-principles molecular-dynamics simulations (5). The electronic structure was treated through the Kohn–Sham formulation of density-functional theory (DFT) (6), using the generalised-gradient approximation (GGA) with the Perdew–Burke–Ernzerhof (PBE) exchange–correlation functionals (7). The CP2K code uses a Gaussian basis set with an auxiliary plane-wave basis set (8). All atomic species were represented by using a triple-ζ valence-polarised (TZVP) Gaussian basis set (9) in conjunction with the Goedecker–Teter–Hutter (GTH) pseudopotential (10). Four, five and six valence s and p electrons were considered for Ge, Sb and Te, respectively. The plane-wave energy cut-off was set to 400 Ry to efficiently solve the Poisson equation within the Quickstep approach (5).

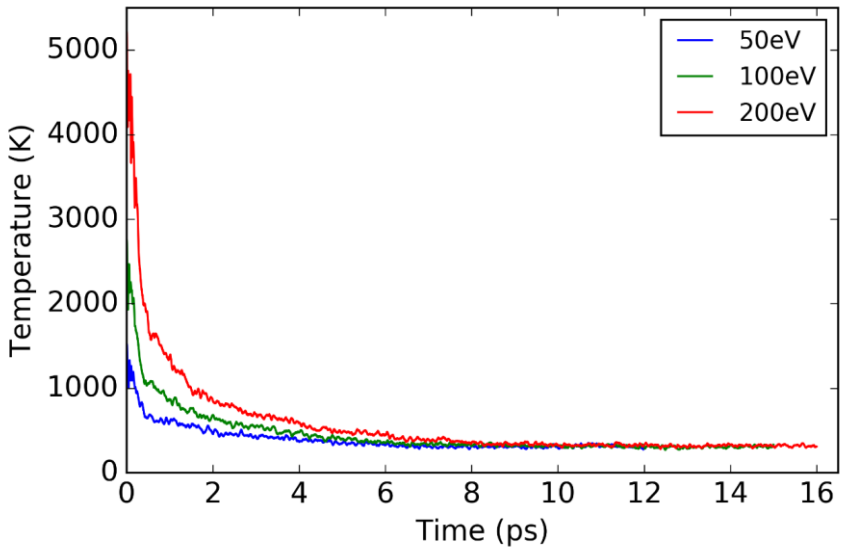

Fig. S2. Temporal evolution of the temperature of the amorphous $Ge_2Sb_2Te_5$ system during the ion-irradiation simulation for the three different thermal-spike energies modelled in this work. The system follows a Newtonian cooling process and hence the radiation-damage cascade acts as a fast thermal quench.

The behavior of the total radial distribution function over time during the 200eV ion-irradiation simulation was investigated and presented in **Fig. S3**. The evolution of g(r) was estimated by averaging over 0.1ps (or 0.2ps) along the molecular-dynamics trajectory and three distinct time domains can be identified. Up to ~ 0.2ps, the total radial distribution function of the modelled system remains similar to that of the initial amorphous structure, highlighting no significant changes in the amorphous network. However, as the radiation-damage cascade evolves inside the glass structure, the calculated g(r) of the system for time intervals between 0.2 and 3.0 ps shows a different behavior. The heights of peaks, notably the second and third peaks, appear to be lower and their shapes become almost featureless, as can be seen in the top panel of **Fig. S3**. The observed changes in the total radial distribution function can be attributed to the partial local melting of the 225GST glass structure due to the damage imposed by the thermal-spike. The calculated pair correlation function for time intervals of the MD trajectory after ~ 4ps seems to become similar again to that of the amorphous 225GST. It can be noted that any time domain after 3ps of the ion-irradiation simulation corresponds to a model temperature much below the melting temperature of the glass structure (~ 900K). This reversible behavior of the calculated g(r) along the molecular-dynamics trajectory is indicative of the recovery of the amorphous network, since the short-range-order structure of the irradiated model reverts back to the solid amorphous phase.

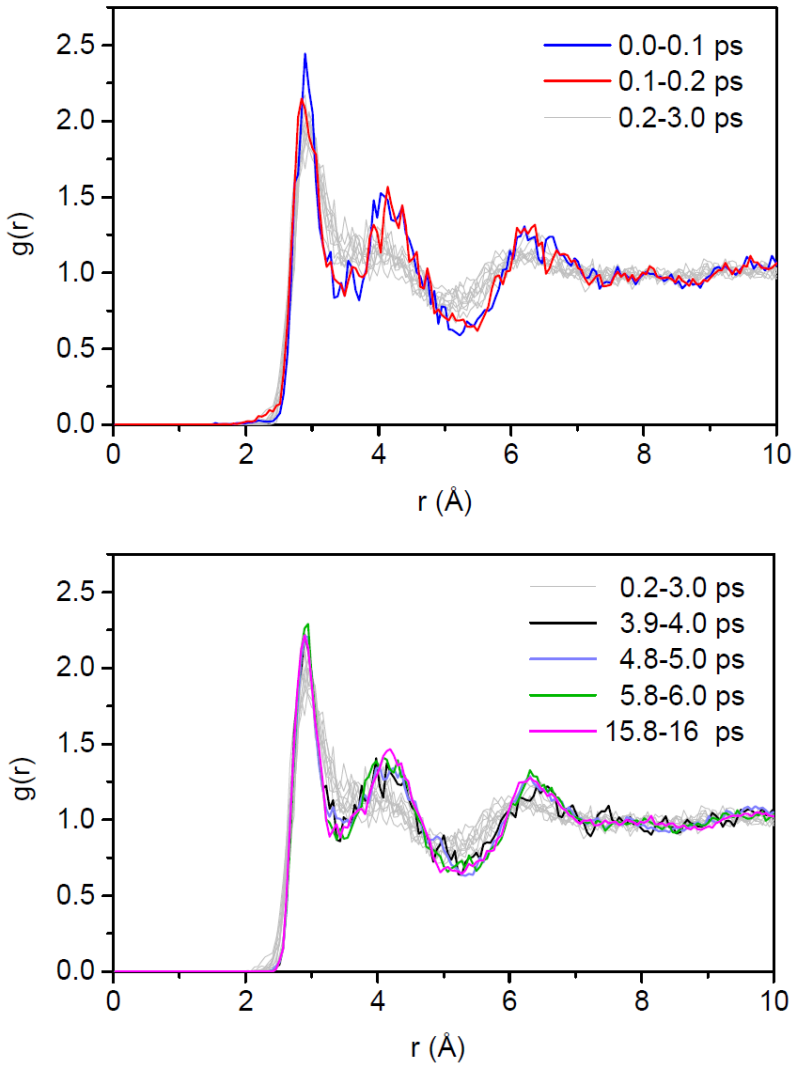

Fig. S3. The temporal change in the total radial distribution function of the modelled system during the 200eV ion-irradiation simulation. The evolution of g(r) was estimated by averaging over 0.1ps (or 0.2ps) along the molecular-dynamics trajectory. No significant changes can be observed in the total g(r) of the glass model in the first 200fs of the simulation. In the time domain 0.2 - 3.0ps, the behaviour of the RDF highlights the damage that the thermal-spike caused in the glass structure, since there is a loss of definition of the second and third coordination shells. However, the calculated RDF for time intervals after 4ps shows the recovery of the glass network and is characteristic of the radiation-tolerance of the amorphous 225GST.

The ring-size distribution for the liquid state of the 315-atom structural model of 225GST, which was used as an initial structure to perform the radiation-damage simulations, was calculated and is presented in **Fig. S4**. It is noted that the liquid structure was generated by *ab initio* molecular-dynamics simulation at a temperature of 1200 K and further computational details

can be found in Ref. (11). For purposes of comparison, the distribution of the shortest-path rings was estimated following the same approach as the one that was used for the data presented in **Fig. 4*A***, i.e. using the Franzblau algorithm with a bonding cut-off distance of 3.2 Å.

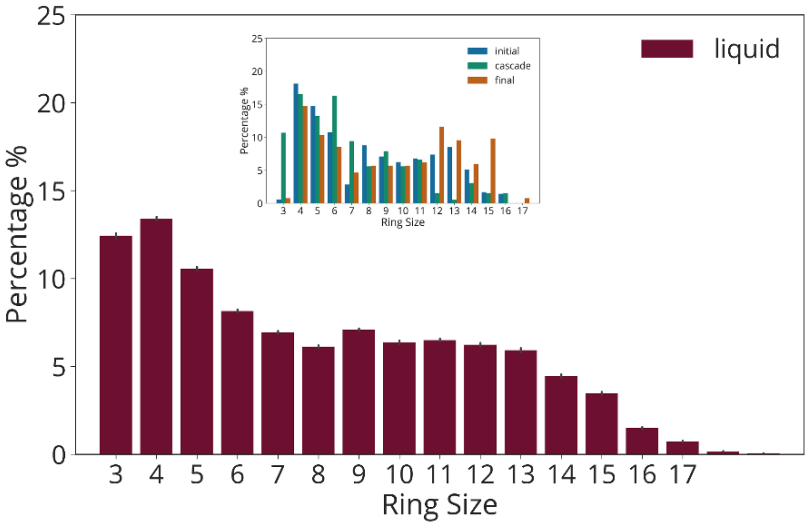

Fig. S4. Ring-size distribution in liquid $Ge_2Sb_2Te_5$. The shortest-path rings were calculated in the liquid phase of a 315-atom model generated by *ab initio* molecular-dynamics simulation at 1200 K. It can be observed that 7–12 fold rings have an almost uniform distribution, which agrees well with the similar pattern observed in the ring-size distribution of the final equilibrated glass model after the radiation-damage cascade. This comparison highlights the more "liquid-like" character of the irradiated $Ge_2Sb_2Te_5$ glass model. Inset: **Fig. 4*A*** from the main text.

In **Fig. 4*B***, the Voronoi-tesselation approach of vacant and atomic centres was used to estimate the temporal evolution of the volume of vacancies inside the glass structure for the 200 eV ion-irradiation simulation. It can be noted that this approach calculates, relatively accurately, the vacant volumes for amorphous and cubic crystalline 225GST and it has been used successfully in previous studies by our group (12).

A different approach was also employed to calculate the evolution of the vacant volume in the modelled system. In the second approach, atomic and non-atomic (i.e. vacant) volumes were assigned by drawing a sphere around each atom. A geometric space that is within 2.5 Å of the nearest atom is labelled as an atomic volume for each atom. By integrating all such volumes for the atoms inside the glass structure, a total atomic volume can be computed.

The non-atomic volume is then simply defined as the difference between the total volume and the atomic volume. Although, with the second approach, a much smaller vacancy volume is

estimated compared with that obtained by the Voronoi-tesselation approach, the trend of vacancy-volume change as a function of time during the ion-irradiation simulation is more clearly highlighted, as shown in **Fig. S5**. It can be observed that the large vacant sites survived only for less than 1ps. In addition, the recovery of the amorphous network is prominently highlighted during the molecular-dynamics simulation.

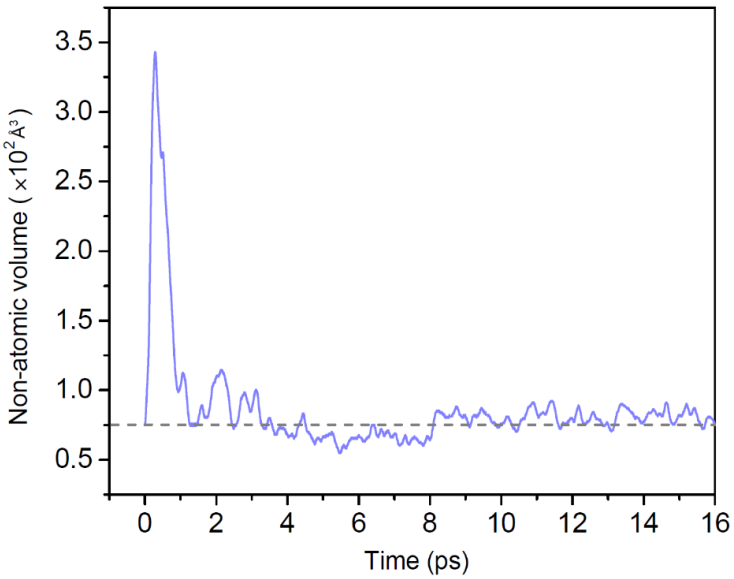

Fig. S5. The temporal change of the vacant volume within the amorphous 225GST network for the 200 eV thermal-spike simulation. It can be observed that the large vacant sites survived only for less than 1ps. The number and size of smaller vacant sites exhibit rather large fluctuations. Overall, the structure shows a recovery back to the initial estimate of the volume of the atomic vacancies within the glass network (indicated with the dashed line).

A zoom in for **Fig. 6*A*** around the Fermi level of the glass models, together with the projection of the DOS onto atomic states of the different species (PDOS), shown in the two figures below for the two glasses before and after irradiation, do not reveal any major differences.

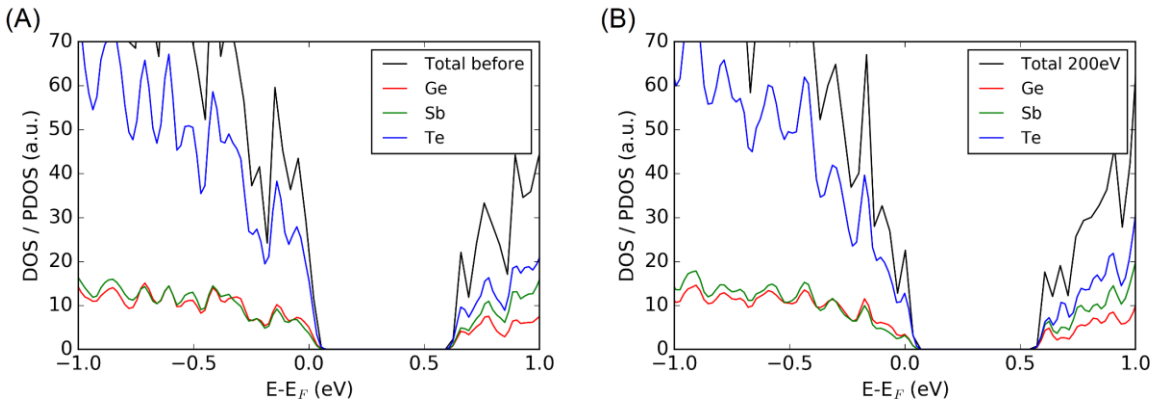

Fig. S6. Total and partial electronic densities of states near the top of the valence band and the bottom of the conduction band for the 225GST glass structure: (A) before irradiation and (B) exposed to the 200eV radiation-damage cascade.

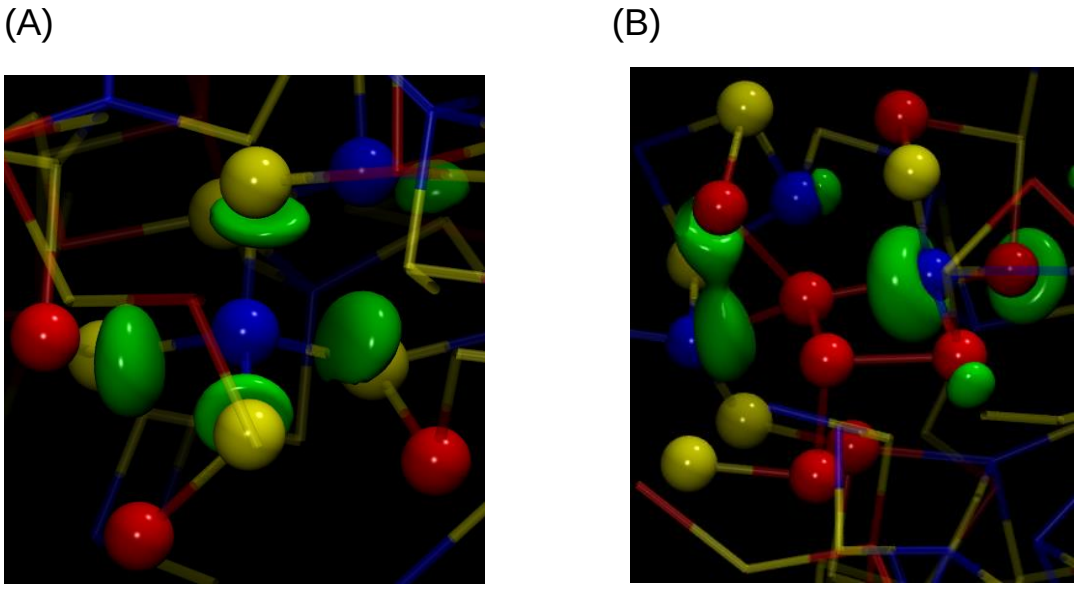

Fig. S7. (A) The lowest unoccupied electronic state (LUMO) in the glass model before the ion-irradiation simulations. The state at the bottom of the conduction band is localized on a $GeTe_4$ tetrahedral unit within the glass network. (B) The lowest unoccupied electronic state (LUMO) in the glass sample after equilibration of the 200 eV thermal-spike simulation. The state at the bottom of the conduction band is localized on a cluster of Ge and Sb atoms. Ge atoms are blue, Sb are red, and Te are yellow. The green isosurfaces, in both configurations, depict the lowest unoccupied molecular-orbital wavefunction amplitude of the system and are plotted with an isovalue of 0.02.

In order to examine if the quenching of the glass to 0K affects the calculated electronic structure of the irradiated model, we computed the displacements of all 315 atoms of the glass structure between the atomic configurations of the final equilibrated irradiated sample at 300K (for the 200eV ion-irradiation simulation) and the geometry of the amorphous 225GST at 0K. The calculated atomic displacements are shown in **Fig. S8**, and it can be observed that each atom has moved less than 1.5 Å upon cooling to 0K. Consequently, since the atoms have not moved within the amorphous network for distances longer than the typical bond lengths between the atomic species in 225GST, the atomic geometry of the glass structure at 0K is not expected to be significantly different than that at 300K, and thus the electronic structure would be similar for both configurations without this quenching affecting the electronic properties of the glass.

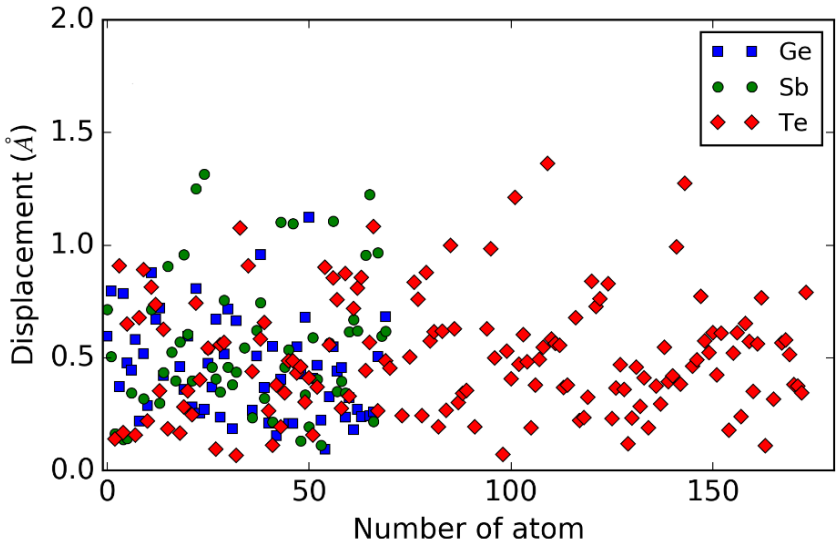

Fig. S8. Atomic displacements for Ge, Sb and Te atoms between the geometry of the final equilibrated irradiated glass structure at 300K (for the 200eV ion-irradiation simulation) and the geometry of the glass model after the quenching to 0K. There are no significant movements of the atoms upon cooling.

In addition, the electronic structure of the final equilibrated configuration at 300K, after exposure to the 200eV radiation-damage cascade, was calculated with the same hybrid functional, and compared with the calculated electronic structure of the glass sample at 0K. The total electronic density of states, as shown in **Fig. S9** for the two glass models, does not exhibit any significant differences. This comparison reinforces the assumption that the quenching to 0K does not have any major impact to the glass structure and hence it does not affect the electronic-structure calculations.

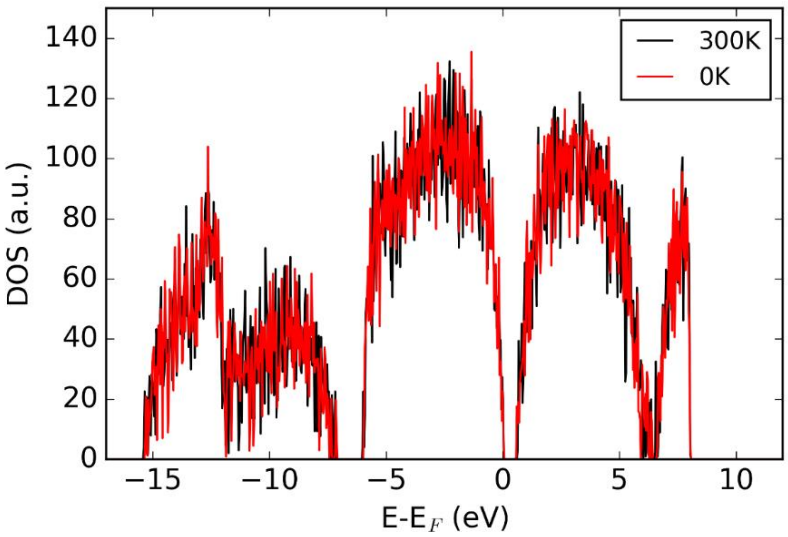

Fig. S9. Total electronic density of states of the amorphous 225GST model at 300K, after the 200eV radiation-damage cascade simulation, and at 0K, after the quenching of the final equilibrated irradiated glass structure. The obtained HOMO-LUMO band gap is 0.64eV and 0.62eV respectively and no significant overall differences can be observed between the electronic structures of the two amorphous models.

References

1. Toton D, Lorenz CD, Rompotis N, Martsinovich N, Kantorovich L (2010) Temperature control in molecular dynamic simulations of non-equilibrium processes. *J Phys: Condens Matter* 22:074205.
2. Kantorovich L, Rompotis N (2008) Generalized Langevin equation for solids. II. Stochastic boundary conditions for nonequilibrium molecular dynamics simulations. *Phys Rev B* 78:094305.
3. Allen MP, Tildesley DJ (1991) Computer simulation of liquids. *Oxford University Press: New York*.
4. Dunn AR, Duffy DM (2011) A molecular dynamics study of diamond and graphite under tritium bombardment. *J Appl Phys* 110:104307.
5. VandeVondele J, Krack M, Mohamed F, Parrinello M, Chassaing T, Hutter J (2005) QUICKSTEP: Fast and accurate density functional calculations using a mixed Gaussian and plane waves approach. *Comput Phys Commun* 167:103–128.
6. Kohn W, Sham LJ (1965) Self-consistent equations including exchange and correlation effects. *Phys Rev Lett* 140:A1133.
7. Perdew JP, Burke K, Ernzerhof M (1996) Generalized gradient approximation made simple. *Phys Rev Lett* 77:3865–3868.

8. Lippert G, Hutter J, Parrinello M (1997) A hybrid Gaussian and plane wave density functional scheme. *Mol Phys* 92:477–487.
9. VandeVondele J, Hutter J (2007) Gaussian basis sets for accurate calculations on molecular systems in gas and condensed phases. *J Chem Phys* 127:114105.
10. Goedecker S, Teter M, Hutter J (1996) Separable dual-space Gaussian pseudopotentials. *Phys Rev B* 54:1703–1710.
11. Lee TH, Elliott SR (2017) The relation between chemical bonding and ultrafast crystal growth. *Adv Mater* 29:1700814.
12. Lee TH, Elliott SR (2011) Structural role of vacancies in the phase tranistion of $Ge_2Sb_2Te_5$ memory materials. *Phys Rev B* 84:094124.